Polarization conversion spectroscopy of hybrid modes

A. Yu. Nikitin,[1,2,*] David Artigas,[3,4] Lluis Torner,[3,4] F. J. García-Vidal,[5] and L. Martín-Moreno[1]

[1]*Instituto de Ciencia de Materiales de Aragón and Departamento de Física de la Materia Condensada, CSIC-Universidad de Zaragoza, E-50009, Zaragoza, Spain*
[2]*A. Ya. Usikov Institute for Radiophysics and Electronics, Ukrainian Academy of Sciences, 61085 Kharkov, Ukraine*
[3]*ICFO–Institut de Ciencies Fotoniques, Mediterranean Technology Park, 08860 Castelldefels (Barcelona), Spain*
[4]*Department of Signal Theory and Communications, Universitat Politécnica de Catalunya, 08034 Barcelona, Spain*
[5]*Departamento de Física Teórica de la Materia Condensada, Universidad Autónoma de Madrid, E-28049 Madrid, Spain*
*Corresponding author: alexeynik@rambler.ru

Enhanced polarization conversion in reflection for the Otto and Kretschmann configurations is introduced as a new method for hybrid-mode spectroscopy. Polarization conversion in reflection occurs when hybrid modes are excited in a guiding structure composed of at least one anisotropic medium. In contrast to a dark dip, in this case modes are associated with a peak in the converted reflectance spectrum, increasing the detection sensitivity and avoiding confusion with reflection dips associated with other processes, such as transmission.
© 2009 Optical Society of America

OCIS codes: 260.1180, 260.5430, 240.6690, 230.5440, 160.1190.

Waves incident on the surface of an anisotropic medium can be reflected with a polarization orthogonal to the incident one [1]. In natural crystals, this conversion of polarization states is small for incidence below the critical angle [2] and increases under total reflection conditions [3]. Total conversion has been predicted in corrugated structures [4] and in metallic interfaces supporting plasmons [5–7]. Structures using anisotropic thin films have shown an enhancement of this polarization conversion [8]. Of importance, similar structures can support different kinds of hybrid guided modes. A special case includes surface waves (SWs) supported at the interfaces between anisotropic and isotropic media [9]. These SWs, referred to as Dyakonov SWs, are hybrid waves existing under special conditions that have been recently observed thanks as a result of the polarization conversion effect in the Otto–Kretschmann excitation scheme [10]. Under this scheme, the usual dip in a bright background observed in reflection (conserving polarization) was replaced by a bright peak in a dark background for the orthogonal polarization. Additionally, reflection dips that are not associated with modes of the structure, as can be transmission, did not result in a peak in the polarization-converted image. This provided a higher contrast and specificity, making possible the observation of Dyakonov SWs.

In addition to increasing contrast, the results in [7,8,10] suggest that in the Otto–Kretschmann configuration, the hybrid nature of any existing mode is related to the enhanced polarization conversion effect. The aim of this Letter is to theoretically demonstrate that the mode excitation is related to polarization conversion that can be used as a new method for hybrid mode spectroscopy.

Consider a plane arbitrarily polarized monochromatic wave with the wave vector $\mathbf{k}_{inc}$ incident from a prism with dielectric permittivity ϵ on a uniaxial crystal characterized by a dielectric tensor $\hat{\epsilon}$ with lon-

gitudinal $\epsilon_\parallel$ and orthogonal $\epsilon_\perp$ components. The Otto (O) geometry is achieved when the uniaxial crystal is separated from the prism by a dielectric medium (gap) of width ℓ and permittivity ϵ_g [Fig. 1(a)]. The Kretschmann (K) geometry is obtained when the crystal with thickness ℓ is sandwiched between the prism and the dielectric medium [Fig. 1(b)]. The labo-
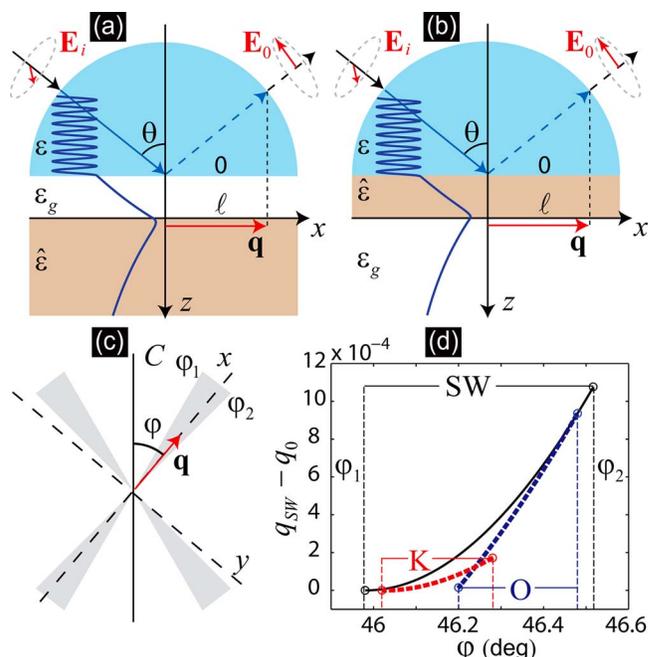

Fig. 1. (Color online) Geometry of the studied systems corresponding to the (a) O and (b) K configuration. (c) Dashed sectors schematically show the values of angle φ at which Dyakonov SWs exist. (d) Effective index q_{SW} in the range of SW existence for the original Dyakonov (solid curve), O (dashed curve as marked), and K (dashed curve as marked) configurations for the following parameters: $\epsilon_g = 4.41$ (Ta_2O_5), $\epsilon = 6.7$ (ZnSe), $\epsilon_\perp = 3.97$, $\epsilon_\parallel = 4.9$ (YVO$_4$), $\ell = 4\lambda$, $q_0 = \sqrt{\epsilon_g}$.

© 2009 Optical Society of America

ratory axes are chosen so that the axis z is orthogonal to the media interfaces and the axis x is oriented at an angle φ relative to the optic axis C of the crystal. The interface of the prism coincides with the $z=0$ plane. The electric field in the prism is written in a compact form as

$$\mathbf{E}_m(\mathbf{r}) = \sum_\sigma \mathbf{e}_i^\sigma E_i^\sigma e^{i\mathbf{k}_{inc}\mathbf{r}} + \sum_{\sigma,\sigma'} \mathbf{e}_r^\sigma R_r^{\sigma\sigma'} E_i^{\sigma'} e^{i\mathbf{k}_r\mathbf{r}}. \quad (1)$$

Here $\sigma=s(p)$ specifies the polarization. The index i is related to the incident wave. E_i^σ are the polarization amplitudes of the incident wave, and r stands for the reflected one; $R_r^{\sigma\sigma'}$ are the reflection coefficients (RCs). The polarization vectors are $\mathbf{e}^s=\mathbf{e}^y$ and $\mathbf{e}^p=\mathbf{e}^s \times \mathbf{q}/q$, where $\mathbf{q}=\mathbf{k}_t/g$ is the dimensionless wave vector component parallel to the interface, and $g=\omega/c$. In the laboratory coordinate system $q=\sqrt{\epsilon}\sin\theta$, θ being the incidence angle. The fields inside the isotropic gap (in the case of the O geometry) and inside the substrate (for the K geometry) are decomposed using the same polarization basis. Inside the crystal the unit vectors for the extraordinary and ordinary waves are $\mathbf{e}^e=\epsilon_\perp\mathbf{e}^x-(\mathbf{e}^x\cdot\mathbf{q}_e)\mathbf{q}_e$ and $\mathbf{e}^o=\mathbf{e}^C\times\mathbf{q}^o$, respectively. The z components of the dimensionless wave vectors $q_{z\alpha}=k_{z\alpha}/g$, where α specifies the medium, are $q_{zi}=-q_{zr}=\sqrt{\epsilon}\cos\theta$, $q_{zg}=\pm\sqrt{\epsilon_g-q^2}$, $q_{zo}=\pm\sqrt{\epsilon_\perp-q^2}$, $q_{ze}=\pm\sqrt{\epsilon_\parallel-q^2[\sin^2\varphi+(\epsilon_\parallel/\epsilon_\perp)\cos^2\varphi]}$. The sign choice depends on the propagation direction of the corresponding wave.

By matching the tangential components of the fields at the boundaries $z=0$ and $z=\ell$, we arrive at the system of linear equations for the unknown RCs. Then the eigenmodes of the system are the solutions of the homogeneous system of equations, when $E_i^\sigma=0$. The mode dispersion relation is obtained from the zeros of the determinant of the system. These equations reduce to the solution for the surface waves studied by Dyakonov [9] in the limit $\ell\to\infty$. Recall that these hybrid SWs (with purely imaginary

q_{zg}, q_{zo}, and q_{ze} for the given q) exist in a certain range of angles φ under the condition $\epsilon_\parallel>\epsilon_g>\epsilon_\perp$ [Figs. 1(c) and 1(d)]. An incident wave from one of the half-spaces cannot couple to the SW directly, since the phase velocity of the SW is less than that of the incident wave. The O and K configurations solve the problem by adding a prism with $\epsilon>\epsilon_g,\epsilon_\parallel,\epsilon_\perp$. Now, the radiation leakage is added to the SW, and the wave incident from the prism at angles exceeding the total internal reflection one, $\cos\theta>\sqrt{\epsilon_g/\epsilon}$, can couple to the SW [Figs. 1(a) and 1(b)]. However, the radiation leakage restricts the angular interval of the SW existence. For the O configuration the dispersion curve is mainly cut from the lower angles, while for the K geometry the curve is cut from the higher angles.

Returning to the inhomogeneous case, we would like to emphasize that—as follows directly from the system of equations—$|R_r^{sp}|=|R_r^{ps}|$ and $|R_r^{ss}|=|R_r^{pp}|$ when the fields are evanescent both in the isotropic media and in the crystal. Thus, the reflection of the plane wave is symmetric relative to the polarizations of the incident and reflected waves. An example of the SW excitation for a YVO$_4$ crystal is shown in Fig. 2. For this crystal, and using Ta$_2$O$_5$ as the isotropic medium, the pure Dyakonov SW exists in the angular range $\varphi\in[45.98°,46,52°]$. The vertical arrows in both (a) and (b) indicate the positions of the angle for the pure Dyakonov SW ($q=q_{SW}$), leaky Dyakonov SW ($q=q_{LSW}$), and the branch points for both the extraordinary wave, $q_{ze}=0$, and the isotropic medium, $q_{zg}=0$. The branch point of the ordinary wave, $q_{zo}=0$, is far below the interval of incidence angles θ shown in the figure. The spectral position of the leaky Dyakonov SW virtually coincides with the angle of RCs maximum, where enhanced polarization conversion takes place [Figs. 2(a) and 2(b)]. The width of the resonance curve depends on the gap thickness as shown in Figs. 2(c) and 2(d). For each fixed θ there is an optimal value of ℓ corresponding to the best compromise between coupling strength and radiation
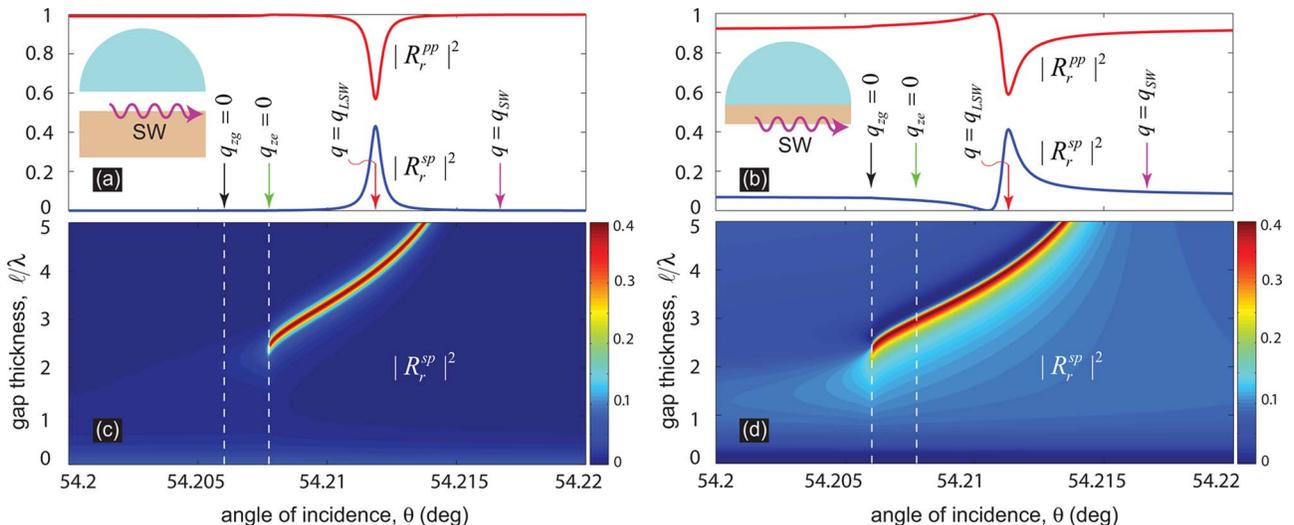

Fig. 2. (Color online) (a), (b) Squared modulus of the polarization RCs as functions of the incidence angle θ for a gap thickness $\ell=4\lambda$ and for $\varphi=46.25°$. (a) is for O configuration, (b) is for K configuration. (c) and (d) render the contour plot for the cross-polarization RCs squared modulus as a function of both θ and ℓ. All parameters are the same as in Fig. 1.

leakage. Interestingly, when ℓ increases, the required angle of incidence evolves toward the value corresponding to the pure Dyakonov SW, demonstrating that polarization conversion is related to the hybrid mode in the structure.

The transformation process and excitation of the SW can be visually demonstrated by plotting the instant spatial field distribution (Fig. 3). In this figure we show two projections of the electric field when the incident wave is s polarized (incident field with y component only) in the O configuration. The two upper insets show the nonresonant case, when the SW is not excited. Here a strong internal reflection takes place, resulting in an interference pattern for the E_y component. In this case, which does not show polarization conversion, all the fields below the prism are evanescent, and inside the crystal they are distributed between the ordinary and extraordinary components. Under the resonant conditions, shown in two lower insets, the increase of the field amplitude at the boundary between the crystal and the gap demonstrates the excitation of the SW. This is connected with a reduction in the y component of the reflected wave (resulting in a lower contrast interference pattern) that is converted into the orthogonal polarization, leading to a strong reflection in the E_z component.

The central point of this Letter is that polarization conversion spectroscopy is restricted not only to Dyakonov surface waves, but to other structures supporting hybrid modes. For example, Fig. 4 shows polarization conversion for the simpler case of a waveguide, where four peaks corresponding to the two first TE- and TM-dominant hybrid modes are clearly shown. Polarization conversion has also been experimentally observed in a more complex situation in-

Fig. 4.   (Color online) Reflection coefficients for hybrid-mode spectroscopy in a waveguide in K geometry with $\ell = 0.7\lambda$, $d = \lambda$, $\epsilon_d = 5.5$, and ϵ_g, ϵ, $\hat{\epsilon}$ as in Fig. 1. The inset represents the zoom of the highlighted region with $\Delta\theta = \theta - \theta_0$ and $\theta_0 = 58.497°$.

volving metals [7], where the excited plasmon was a hybrid SW that was mainly a TM mode [11].

These results demonstrate the link between excitation of hybrid modes and enhanced polarization conversion in Otto–Kretschmann geometries. However, note that analogous resonance effects take place when hybrid modes are excited not by a prism but by a periodical structure formed on the surface of the crystal. In that case the polarization conversion can be observed both in the zeroth and higher diffraction orders. As a result, polarization conversion can be used in all these configurations as a new hybrid-mode spectroscopic method.
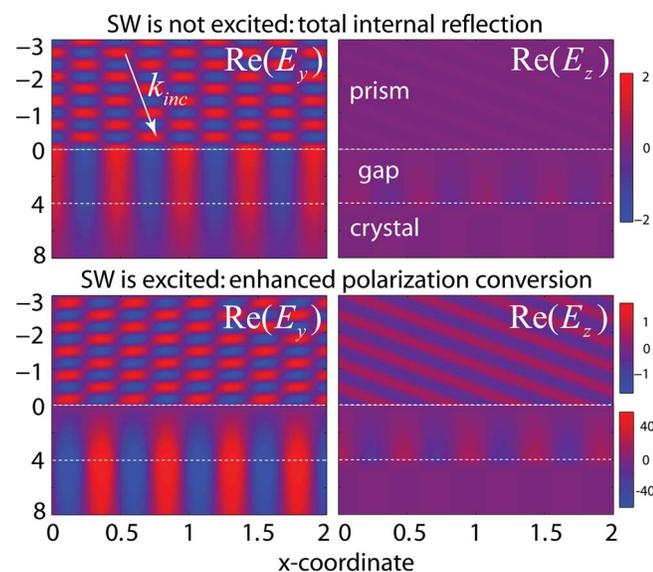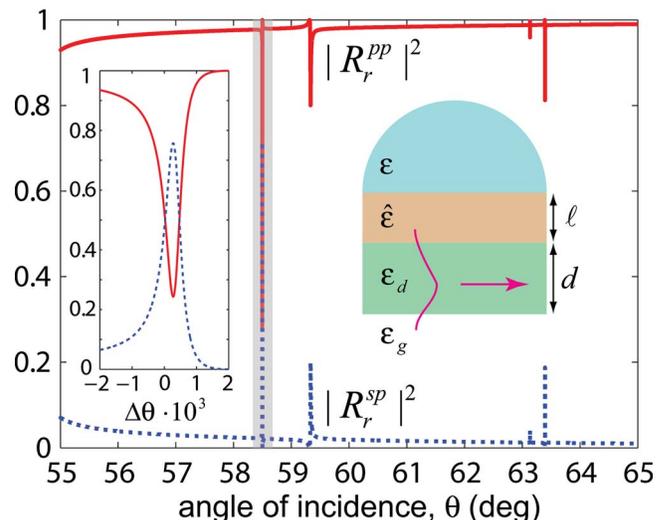
Fig. 3.   (Color online) Spatial distribution of the real part of the electric field in the O configuration. The calculations for the upper panels are done at $\theta = 54.23°$, while for the lower panel the incidence angle is $\theta = 54.212°$. In all panels $\varphi = 46.25°$ and ϵ_g, ϵ, $\hat{\epsilon}$, ℓ are the same as in Fig. 1.

References

1. J. Lekner, J. Phys. Condens. Matter **3**, 6121 (1991).
2. J. Lekner, J. Phys. Condens. Matter **4**, 9459 (1992).
3. F. Yang and J. R. Sambles, J. Mod. Opt. **40**, 1131 (1993).
4. R. A. Depine and M. I. Gigli, Phys. Rev. B **49**, 8437 (1994).
5. G. P. Bryan-Brown, J. R. Sambles, and M. C. Hutley, J. Mod. Opt. **37**, 1227 (1990).
6. A. V. Kats, M. L. Nesterov, and A. Yu. Nikitin, Phys. Rev. B **72**, 193405 (2005).
7. Y. J. Jen and C. L. Chiang, Appl. Phys. Lett. **94**, 011105 (2009).
8. Y. J. Jen and C. L. Chiang, Opt. Commun. **265**, 446 (2006).
9. M. I. D'yakonov, Sov. Phys. JETP **67**, 714 (1988).
10. O. Takayama, L. Crasovan, D. Artigas, and L. Torner, Phys. Rev. Lett. **102**, 043903 (2009).
11. D. Mihalache, D. M. Baboiu, M. Ciumac, L. Torner, and J. P. Torres, Opt. Quantum Electron. **26**, 857 (1994).